



Investigation of the steam reforming of a series of model compounds derived from bio-oil for hydrogen production

Xun Hu^{a,b}, Gongxuan Lu^{a,*}

^a State Key Laboratory for Oxo Synthesis and Selective Oxidation, Lanzhou Institute of Chemical Physics, Chinese Academy of Sciences, Lanzhou 730000, PR China

^b Graduate School of Chinese Academy of Sciences, Beijing 100039, PR China

ARTICLE INFO

Article history:

Received 21 August 2008

Received in revised form 16 October 2008

Accepted 31 October 2008

Available online 6 November 2008

Keywords:

Steam reforming

Hydrogen

Bio-oil

Coke formation

ABSTRACT

In this study, steam reforming of acetic acid, ethylene glycol, acetone, ethyl acetate, m-xylene, and glucose, which were representative of the main components in bio-oil, were performed to investigate the feasibility of these feedstocks for hydrogen production. The effects of reaction temperature and steam to carbon ratios (S/C) on steam reforming as well as coke formation tendency of the bio-oil components in the presence and absence of steam were investigated in a detailed manner. Low reaction temperature and S/C led to low steam reforming efficiency, and consequently decomposition or degradation of the feedstocks dominated, resulting in large amounts of by-products. Increasing reaction temperature and S/C increased the steam reforming rates and the partial pressure of steam on catalyst surface, favoring conversion of the feedstocks and removal of the by-products. Coke formation rates of the feedstocks during the long-term experiments decreased in the following orders: glucose \gg m-xylene $>$ acetone $>$ ethyl acetate $>$ ethylene glycol $>$ acetic acid. Decomposition or polymerization of the feedstocks to carbonaceous deposit was the main route for coke formation in glucose, m-xylene, and acetone reforming, while the large amounts of by-products such as ethylene, CO, or acetone were main sources of coke in the steam reforming of ethyl acetate, ethylene glycol, and acetic acid.

© 2008 Elsevier B.V. All rights reserved.

1. Introduction

Presently, hydrogen production has attracted great interest in energy area because of its potential application in the transportation and the production of electricity with fuel cell systems [1,2]. The traditional processes for hydrogen production are the catalytic steam reforming of natural gas, light hydrocarbons, and naphtha, or gasification of coal to yield syngas followed by water gas shift conversion [3,4]. These methods are commonly used and are generally considered as the economically competitive ways for hydrogen production [5]. However, both the hydrocarbons and coal are the kinds of fossil fuels, and their usage fails to provide a solution to deal with the huge amount of carbon dioxide emissions during the reforming processes [6]. On the other hand, shortage of fossil fuel in the near future will cause serious energy problems. Therefore, the development of the technology utilizing biomass energy resources to produce hydrogen attracts much attention, due to the renewable, available, and carbon-neutral features of biomass [7,8].

Much experimental and modelling work has been performed to date on converting biomass to hydrogen using different thermo-

chemical pathways, mostly involving gasification or pyrolysis of biomass at various temperatures and pressures [9,10]. The promising biomass-hydrogen option is the flash pyrolysis of biomass to bio-oil and followed steam reforming [11]. Bio-oil is a mixture of oxygenated compounds including acids, alcohols, ketones, esters, ethers, aldehydes, phenols, and derivatives, as well as carbohydrates, and a large proportion (20–30 wt.%) of lignin-derived oligomers [12]. By the addition of water, bio-oil can be separated into a hydrophobic-lignin derived fraction and an aqueous fraction (50 wt.% of the bio-oil) containing mostly carbohydrate-derived monomeric compounds [13]. Steam reforming of the single compound in the aqueous fraction of bio-oil has been the subject of many research efforts [6,7,14–23]. Nevertheless, bio-oil is a complex mixture of various types of organic compounds, and the compounds contain distinct molecular structure that may greatly affect the product distribution and coke formation in steam reforming process. Therefore, steam reforming of bio-oil as a whole requires a thorough understanding about the behavior of the various bio-oil components in steam reforming process.

With this background, a systematic and detailed comparison of steam reforming of a series of bio-oil-derived model components, including acetic acid, ethylene glycol, acetone, ethyl acetate, m-xylene, and glucose, were performed in this study. The selected

* Corresponding author. Fax: +86 931 4968178.

E-mail address: gxlu@lzb.ac.cn (G. Lu).

compounds are representative of the organic acids, alcohols, ketones, esters, aromatic compounds, and sugars in bio-oil, respectively. The steam reforming reactions were carried out over a typical reforming catalyst, Ni/Al₂O₃ catalyst, and the influence of the reaction parameters including reaction temperature, steam to carbon ratios (S/C), and reaction time on the steam reforming reactions were investigated. The coke formation tendency of the model compounds in the presence and absence of steam were analyzed in detail, to assess their feasibility for steam reforming.

2. Experimental

2.1. Catalyst preparation

Ni/Al₂O₃ catalyst was prepared by impregnation method using Ni(NO₃)₂·6H₂O as a precursor. The nickel loading was 30 wt.% to Al₂O₃. Before impregnation, the support γ -Al₂O₃ (129 m² g⁻¹, 30–45 mesh) was stabilized in air at 600 °C for 6 h. After impregnation, the catalyst precursors were dried at room temperature for 24 h and at 110 °C for another 24 h. Finally, the precursor was calcined at 500 °C for 4 h. Ni/Al₂O₃ catalyst was characterized by the BET, temperature-programmed reduction (H₂-TPR), temperature-programmed adsorption (H₂-TPD), and X-ray diffraction spectra (XRD) techniques. The physicochemical properties of Ni/Al₂O₃ catalyst are summarized in Table 1.

2.2. Catalytic activity measurements

Catalytic test was carried out at atmospheric pressure in a fixed-bed continuous flow quartz reactor (i.d. 8 mm), consisting of a flow controller unit, a reactor unit, and an analysis unit. A schematic

Table 1

Physicochemical properties of Ni/Al₂O₃ catalyst.

| Sample | Ni/Al ₂ O ₃ |
|--|-----------------------------------|
| Ni loading (wt.%) | 30 |
| Specific surface area ^a (m ² g ⁻¹) | 126.2 |
| V _{pore} ^a (cm ³ g ⁻¹) | 0.28 |
| D _{pore} ^a (nm) | 9.8 |
| D _{red} ^b (%) | 10.9 |
| D _{disp} ^c (%) | 7.8 |
| Ni size ^d (nm) | 23.6 |

^a Data were obtained by the BET method.

^b Reduction degree of Ni: the ratio of reduced Ni to total Ni × 100.

^c Dispersion of metal particles: ((2 × H₂ adsorption)/reduced Ni) × 100.

^d Ni particle size calculated by the Scherrer formula from the X-ray diffraction spectra of the reduced Ni/Al₂O₃ catalyst.

diagram of the experimental system is shown in Fig. 1. Typically, the temperature increased from 300 to 800 °C at a 50 °C increment, and a sample was taken for analysis after stabilizing for 1 h at each investigated temperature. 0.5 g catalyst diluted with equal amount of quartz was used in each run. Prior to the experiment, the calcined catalyst was reduced in situ at 600 °C (heating rate 10 °C/min) for 3 h with a 50 vol.% H₂/N₂ mixture (flow rate: 60 ml/min). The soluble feedstocks (acetic acid, ethylene glycol, acetone, glucose) were firstly dissolved in water with a given steam to carbon ratio (S/C). Then the reaction mixture was fed into the reactor by a syringe pump with a liquid hourly space velocity (LHSV) of 10.1 h⁻¹ using N₂ (40 ml/min) as the carrier gas. The insoluble feedstocks (ethyl acetate, m-xylene) and water were introduced into reactor by two syringe pumps. The total LHSV was regulated at 10.1 h⁻¹ and the S/C was determined according to different runs. Separation and quantification of the gaseous products were attained on two on-line chromatographs (GC) equipped with thermal-conductivity

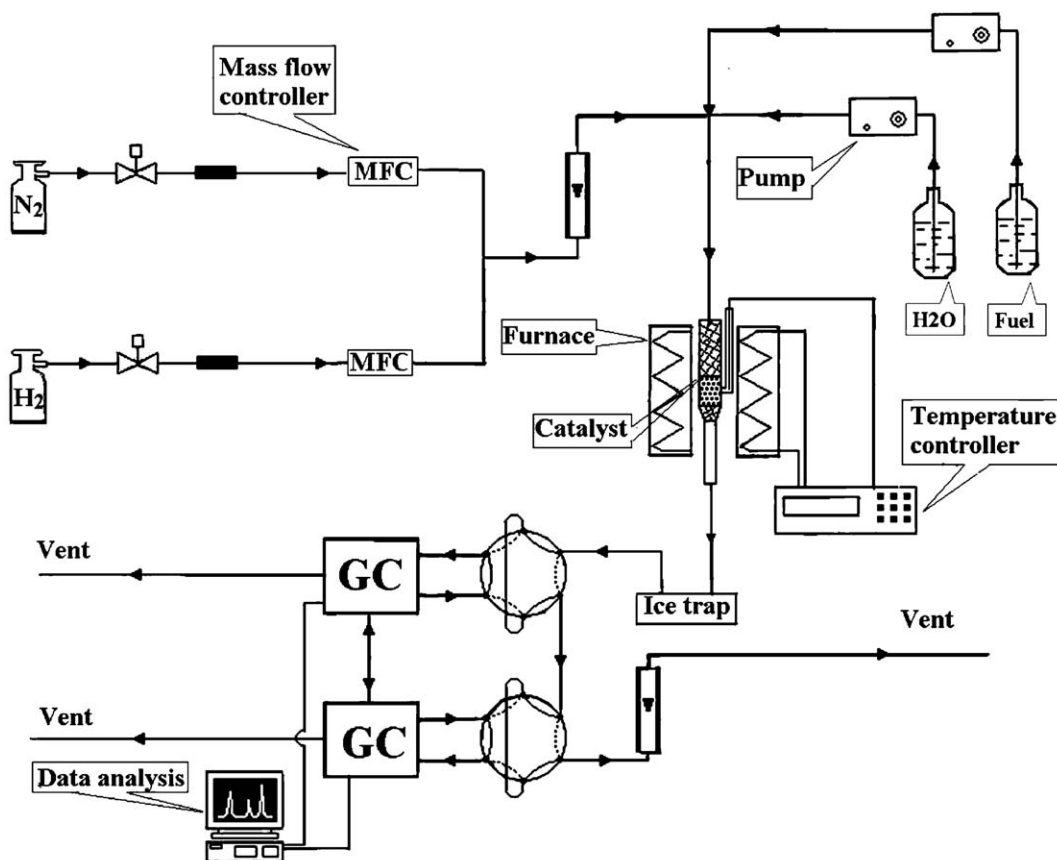


Fig. 1. Schematic diagram of the experimental system.

Table 2

The reactions involved in steam reforming process.

| Reactions involved in steam reforming process | ΔH_{298}° (kJ/mol) |
|---|-----------------------------------|
| <i>Stoichiometry for the “full” steam reforming reactions</i> | |
| $\text{CH}_3\text{COOH} + 2\text{H}_2\text{O} \rightarrow 4\text{H}_2 + 2\text{CO}_2$ (1) | 131.4 |
| $\text{CH}_2\text{OHCH}_2\text{OH} + 2\text{H}_2\text{O} \rightarrow 5\text{H}_2 + 2\text{CO}_2$ (2) | 86.2 |
| $\text{CH}_3\text{COCH}_3 + 5\text{H}_2\text{O} \rightarrow 8\text{H}_2 + 3\text{CO}_2$ (3) | 246.3 |
| $\text{CH}_3\text{COOCH}_2\text{CH}_3 + 6\text{H}_2\text{O} \rightarrow 10\text{H}_2 + 4\text{CO}_2$ (4) | 320.1 |
| $\text{C}_8\text{H}_{10} + 16\text{H}_2\text{O} \rightarrow 21\text{H}_2 + 8\text{CO}_2$ (5) | 738.4 |
| $\text{C}_6\text{H}_{12}\text{O}_6 + 6\text{H}_2\text{O} \rightarrow 12\text{H}_2 + 6\text{CO}_2$ (6) | 364.4 |
| <i>Cracking of the feedstocks and internal conversion of the gaseous products</i> | |
| $\text{C}_n\text{H}_m\text{O}_k \rightarrow \text{C}_x\text{H}_y\text{O}_z + \text{gas} (\text{CO}, \text{CH}_4, \text{CO}_2, \text{H}_2, \dots)$ (7) | – |
| $\text{C}_n\text{H}_m\text{O}_k \rightarrow \text{C}_x\text{H}_y\text{O}_z + \text{H}_2\text{O}$ (8) | – |
| $\text{H}_2 + \text{CO}_2 \rightarrow \text{H}_2\text{O} + \text{CO}$ (9) | 41.1 |
| $\text{CO} + \text{H}_2\text{O} \rightarrow \text{H}_2 + \text{CO}_2$ (10) | –41.1 |
| $\text{CO} + 3\text{H}_2 \rightarrow \text{CH}_4 + \text{H}_2\text{O}$ (11) | –206.2 |
| $\text{CO}_2 + 4\text{H}_2 \rightarrow \text{CH}_4 + 2\text{H}_2\text{O}$ (12) | –165.1 |
| $\text{CH}_4 + \text{H}_2\text{O} \rightarrow \text{CO} + 3\text{H}_2$ (13) | 206.1 |
| $\text{CH}_4 + 2\text{H}_2\text{O} \rightarrow \text{CO}_2 + 4\text{H}_2$ (14) | 165.1 |
| <i>Reactions for coke formation or elimination</i> | |
| $\text{C}_n\text{H}_m\text{O}_k \rightarrow \text{C}_x\text{H}_y\text{O}_z + \text{coke}$ (15) | – |
| $\text{CH}_4 \rightarrow \text{C} + 2\text{H}_2$ (16) | –74.9 |
| $2\text{CO} \rightarrow \text{C} + \text{CO}_2$ (17) | –172.4 |
| $\text{CO} + \text{H}_2 \rightarrow \text{C} + \text{H}_2\text{O}$ (18) | –131.3 |
| $\text{CO}_2 + 2\text{H}_2 \rightarrow 2\text{H}_2\text{O} + \text{C}$ (19) | –90.1 |
| $\text{C} + \text{H}_2\text{O} \rightarrow \text{CO} + \text{H}_2$ (20) | 131.3 |
| $\text{C} + \text{CO}_2 \rightarrow 2\text{CO}$ (21) | 172.4 |

detectors (TCD). Condensable vapors (ethylene glycol, acetaldehyde, water, acetone, etc.) were trapped in a vessel residing in an ice bath, and then the liquid products was withdrawn periodically and analyzed with a flame ionization detector (FID). Error of the GC results typically close within $\pm 4\%$. Conversion of the feedstocks was calculated by dividing the total carbon in products with the carbon in feed. H_2 selectivity was defined as the fraction of H_2 produced with respect to the theoretical “full” conversion of the feedstocks to H_2 according to Eqs. (1)–(6) presented in Table 2. The calculated method of the carbon-containing product's selectivities was defined by the

formula: $S_{\text{carbon-containing product}} (\%) = 100 \times (\text{moles of carbon-containing compounds}) / (\text{moles of carbon reacted})$. The carbon balance was calculated by dividing the total moles of carbon in products with the total moles of carbon reacted. S/C was defined as (moles of steam in feed)/(moles of carbon in feed), while LHSV was defined as volumetric flow rate of feed solution ($\text{cm}^3 \text{h}^{-1}$)/(catalyst bed volume (cm^3)).

2.3. Catalyst characterization

The amounts of carbon deposition on catalyst surface were analyzed by thermo-gravimetric analysis in a PerkinElmer TG/DTA apparatus (Sensitivity: $0.2 \mu\text{g}$). The catalyst was heated from 50 to 800°C at $10^\circ\text{C}/\text{min}$ under synthetic air flow and the mass loss was measured.

3. Results and discussion

3.1. Reactions involved in steam reforming process

For steam reforming reaction, the “full” steam reforming is desired because of the highest hydrogen yield, as presented in Table 2. However, steam-reforming reaction generally involves a complex reaction network due to many pathways for conversion of feedstocks and internal reactions between the primary products, which are summarized as follows.

Many feedstocks in bio-oil are thermally unstable, the homogeneous reactions such as decomposition [Eq. (7)] and dehydration [Eq. (8)] may occur before reaching or on catalyst bed. As a result, undesired organic by-products are produced, which diminishes hydrogen yield.

CO is an intermediate and one of the main by-products in steam reforming process. Low reaction temperature results in low efficiency of steam reforming, and consequently favors the decomposition of the organics [Eq. (7)], leading to a large amount of CO generation. However, high reaction temperature promotes the reverse water gas shift reaction [Eq. (9)], which also results in the production of CO. Conversely, the water gas shift reaction [Eq. (10)] and the methanation of CO [Eq. (11)] contribute to the elimination of CO in mild temperature region [3,24].

Methane, which greatly diminishes hydrogen yield, is another by-product in steam reforming. Decomposition of the organic molecules and methanation of carbon oxides [Eqs. (11) and (12)] are main routes for its formation [2,17,25], while the steam reforming of methane [Eqs. (13) and (14)] contributes to its elimination at high temperatures.

Steam reforming of hydrocarbons involves a risk of carbon deposition, which will cause the loss of the effective surface area, lower the heat-transfer rate from catalyst to gas, or plug the void space within the catalyst [26]. Carbon deposition may arise because of the decomposition of organics [Eq. (15)], CH_4 [Eq. (16)], and disproportion of CO [Eq. (17)] as well as the reaction of CO or CO_2 with H_2 [Eqs. (18) and (19)]. Under a given conditions, steam and carbon dioxide can act as the favorable factors for the elimination of carbon deposit [Eqs. (20) and (21)].

As presented above, there are many routes for conversion of the feedstocks. Nevertheless, the main reaction pathway is determined by the properties of a feedstock and the experimental parameters such as the reaction temperature and S/C, which will be well discussed below.

3.2. Effects of reaction temperature

Steam reforming of the feedstocks was carried out in a wide temperature range of $300\text{--}800^\circ\text{C}$ with an S/C of 6 and a LHSV of 10.1h^{-1} . For comparison, conversions of the feedstocks versus

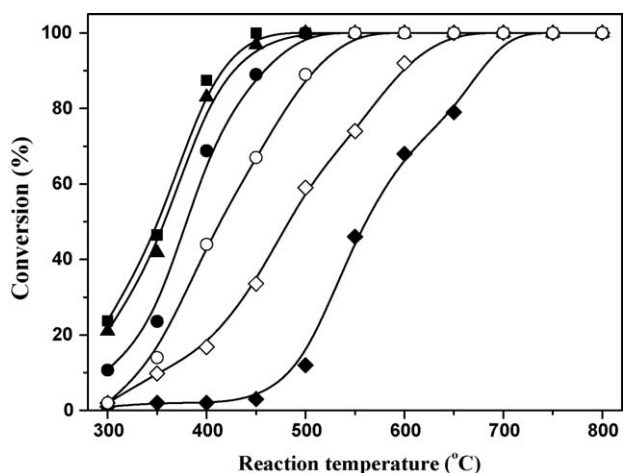


Fig. 2. Conversion of the feedstocks versus reaction temperature: $S/C = 6$; $LHSV = 10.1 \text{ h}^{-1}$; $P = 1 \text{ atm.}$; (■) acetic acid; (▲) ethylene glycol; (●) acetone; (◇) ethyl acetate; (◆) m-xylene; (○) glucose.

reaction temperature were summarized in Fig. 2. The conversion-temperature profiles could approximately be classified into two categories: the light feedstocks (acetic acid, ethylene glycol, acetone) could generally be converted completely in a lower temperature region, and vice versa. Acetic acid was effectively steam reformed at the temperature as low as 400°C , and the followed were acetone and ethylene glycol. The light feedstocks contain short carbon chain, and

therefore less C–C bonds in the molecules needed to be cracked in reforming process. Hence, they were easily reformed. In converse, much higher reaction temperature was required to convert the heavy feedstocks (ethyl acetate, m-xylene, glucose) with the exception of glucose. Although glucose molecule contains six carbon atoms, it could be completely converted at much lower temperature than that of ethyl acetate and m-xylene. Glucose is the oxygenated hydrocarbon that has a C/O ratio of 1. Steam reforming of this type of oxygenated hydrocarbon to CO and H_2 is thermodynamically favorable at significantly lower temperature, which offers a low temperature route for conversion of glucose [27]. Ethyl acetate could be produced from the esterification of acetic acid and ethanol. Therefore, in steam reforming process, ethyl acetate might firstly degrade to acetyl and ethoxy groups that then reacted with the activated steam, as the steam reforming of dimethyl ether [28]. m-Xylene is a tar compound in biomass gasification process [8]. This type of compound contains stable skeleton of benzene ring, destroying of which needs high reaction temperatures. Therefore, low conversion of m-xylene was observed at temperature below 500°C .

Selectivities of the main gaseous products (H_2 , CO_2 , CO, CH_4) versus reaction temperature are summarized in Fig. 3. The gaseous product distributions in steam reforming of the acetic acid, ethylene glycol, and acetone were comparable. The H_2 selectivities increased linearly with the increase of temperature and reached the maximum at 550°C , further increasing reaction temperature resulted in the decrease of H_2 yields. In general, H_2 selectivity was determined by the selectivities toward the by-products such as CO

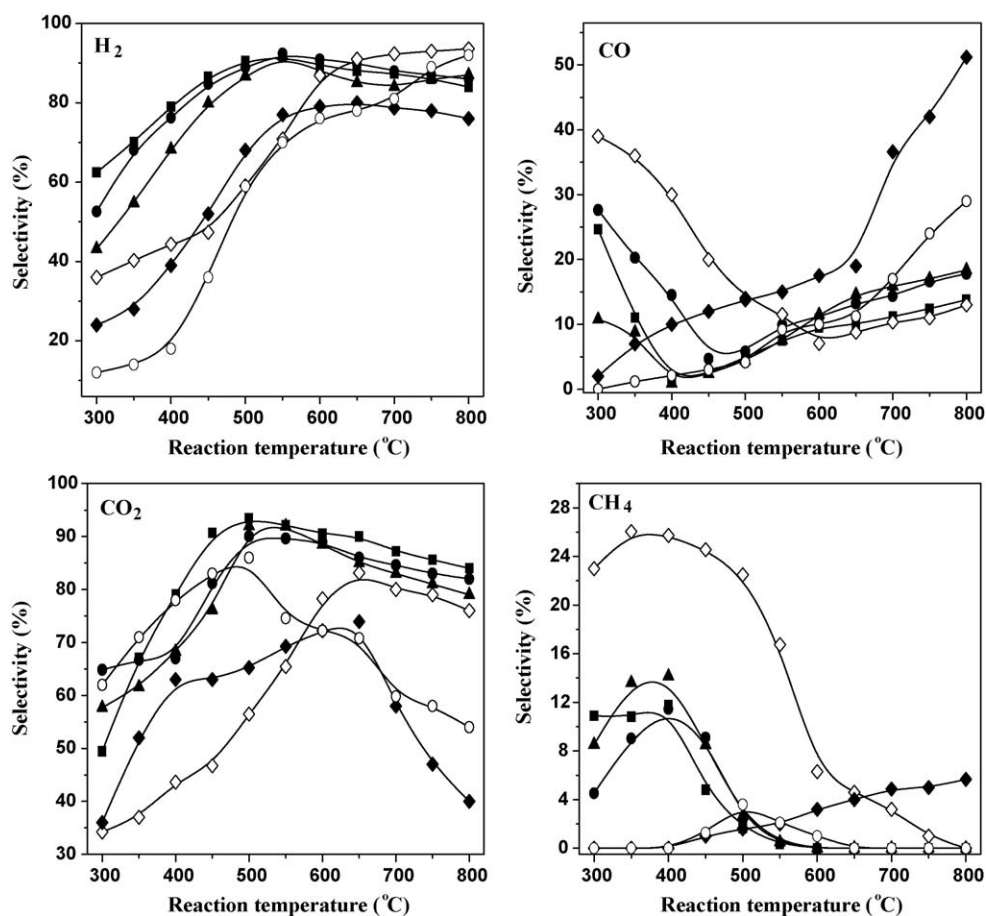


Fig. 3. The gaseous product selectivities versus reaction temperature: $S/C = 6$; $LHSV = 10.1 \text{ h}^{-1}$; $P = 1 \text{ atm.}$; (■) acetic acid; (▲) ethylene glycol; (●) acetone; (◇) ethyl acetate; (◆) m-xylene; (○) glucose.

and CH₄. At the initial reaction temperature (300 °C), steam reforming of the light feedstocks all gave a significant amount of CO because of the low efficiency of both the steam reforming and the water gas shift reaction at this stage. Increasing temperature to 400 °C, steam reforming initiated. CO selectivity decreased drastically while the H₂ and CO₂ selectivities increased correspondingly. However, with the continuous increase of temperature, CO selectivity restarted to increase at the expense of H₂ and CO₂ yields, implying the precedence of the reverse water gas shift reaction at high temperatures. In ethyl acetate reforming process, a very high CO selectivity (up to 40%) was observed at 300 °C, implying the rather low efficiency of Ni/Al₂O₃ catalyst for ethyl acetate reforming at low temperatures. The large amount of CO should come from the decomposition of ethyl acetate, since cracking of both the acetyl and ethoxy groups, which came from decomposition of ethyl acetate, gave the CO intermediate [29,30]. The CO selectivity trends in glucose and m-xylene reforming processes were different from those of others, which increased linearly with the increase of temperature and reached a high level at high temperatures. Obviously, steam reforming of glucose and m-xylene mainly gave CO₂ in low temperature region while gave CO in high temperature region.

CH₄ was another gaseous by-product, which also was produced in a large amount in steam reforming process. Nevertheless, the CH₄ and CO selectivity trends were practically opposite in steam reforming of the light feedstock, as seen in Fig. 2. The production of CH₄ increased quickly with the increase of temperature and went through a maximum at ca. 400 °C, while the further increase of temperature led to the drastic decrease of CH₄ selectivity. Different reaction pathways determined the production of CH₄ in the low, middle, and high temperature regions. Decomposition of the feedstocks might be responsible for CH₄ generation at the low temperatures (300 °C) because of the low efficiency of steam reforming at this stage. Methanation of carbon oxides was speculated as the main reason for the sharp increase of CH₄ amounts at middle temperatures (400 °C), since Ni catalyst

presented high efficiency for methanation of carbon oxides [31,32], and furthermore, the high concentrations of H₂ and CO₂ in effluent gas associated with the mild temperature favored the occurrence of methanation reactions. At higher temperatures, the methanation reactions were suppressed due to the thermodynamic limitation [33]. Moreover, steam reforming of CH₄ initiated at this stage, leading to the drastic decrease of CH₄ selectivity. High CH₄ selectivity was also observed in ethyl acetate reforming process in both the low and middle temperature regions. CH₄ should come from the decomposition of ethyl acetate because the low H₂ yield in the effluent gas limited the occurrence of methanation reactions. In comparison, CH₄ selectivity maintained a low level in both glucose and m-xylene reforming processes at the mild temperatures.

Steam reforming of the feedstocks also gave other organic by-products such as acetone and ketene in acetic acid reforming, ethylene in ethylene glycol reforming, ketene in acetone reforming, ethylene and acetone in ethyl acetate reforming, as well as benzene in m-xylene reforming. The amounts of the organic by-products were significant when the steam reforming reaction was in low efficiency, generally at low reaction temperature. Increasing temperature to high regions, not only the feedstocks but also the organic by-products could be effectively steam reformed, leading to the sharp increase of H₂ yields.

3.3. Effects of the S/C

S/C is another parameter that plays an important role in determining reaction pathways of the feedstocks in steam reforming process. Hence, the effects of S/C that ranged from the stoichiometric ratio up to 9 on steam reforming reactions were investigated. Here the stoichiometric S/C for steam reforming of the feedstocks were calculated according to the “full” steam reforming reactions presented in Table 2. In addition, steam-reforming reactions were performed at 400 °C for the light feedstocks while at 700 °C for the heavy feedstocks, due to low

Table 3

Effects of S/C on feedstocks conversion and gaseous product selectivities—the light feedstocks: $T = 400\text{ °C}$; the heavy feedstocks: $T = 700\text{ °C}$; LHSV = 10.1 h^{-1} ; $P = 1\text{ atm}$.

| Feedstocks | S/C | Conversion (%) | Product selectivity (%) | | | | | Carbon balance (%) |
|-----------------|------|----------------|-------------------------|-----------------|-----------------|------|--------|--------------------|
| | | | H ₂ | CO ₂ | CH ₄ | CO | Others | |
| Acetic acid | 1 | 57.3 | 42.6 | 40.3 | 21.4 | 9.5 | 12.1 | 88.8 |
| | 3 | 70.9 | 61.6 | 54.2 | 17.2 | 8.6 | 10.2 | 90.6 |
| | 6 | 85.4 | 79.1 | 79.7 | 11.7 | 1.1 | 4.6 | 94.3 |
| | 9 | 100 | 90.5 | 91.8 | 1.6 | 0.9 | 0.5 | 99.2 |
| Ethylene glycol | 1 | 46.3 | 55.6 | 43.9 | 15.1 | 16.8 | 8.4 | 89.6 |
| | 3 | 51.8 | 65.0 | 51.3 | 12.5 | 13.2 | 7.7 | 93.1 |
| | 6 | 68.4 | 76.7 | 65.3 | 11.4 | 10.6 | 5.2 | 96.5 |
| | 9 | 96.7 | 89.6 | 84.2 | 5.9 | 3.0 | 1.1 | 98.7 |
| Acetone | 1.67 | 51.1 | 46.5 | 45.3 | 18.8 | 14.1 | 7.6 | 87.6 |
| | 3 | 69.3 | 53.3 | 56.4 | 17.8 | 11.2 | 4.3 | 94.9 |
| | 6 | 82.2 | 68.2 | 76.0 | 14.6 | 1.89 | 1.1 | 97.6 |
| | 9 | 100 | 92.8 | 87.2 | 7.6 | 0.6 | 0.3 | 99.1 |
| Ethyl acetate | 1.5 | 89.1 | 47.7 | 41.8 | 9.6 | 33.4 | 6.1 | 84.8 |
| | 3 | 100 | 55.6 | 57.6 | 5.2 | 28.6 | 3.5 | 87.6 |
| | 6 | 100 | 86.8 | 76.6 | 3.2 | 10.3 | 2.1 | 92.3 |
| | 9 | 100 | 92.5 | 83.0 | 0.6 | 6.7 | 0.4 | 94.8 |
| m-Xylene | 2 | 71.7 | 54.9 | 22.1 | 6.8 | 56.3 | 7.7 | 86.1 |
| | 3 | 77.9 | 64.4 | 27.3 | 5.9 | 48.8 | 6.8 | 92.3 |
| | 6 | 100 | 78.6 | 50.3 | 4.8 | 36.6 | 1.3 | 93.4 |
| | 9 | 100 | 88.9 | 70.7 | 1.7 | 21.7 | 0.2 | 95.1 |
| Glucose | 3 | — | — | — | — | — | — | — |
| | 6 | 100 | 77.1 | 57.2 | 0.9 | 17.7 | 14.4 | 75.2 |
| | 9 | 100 | 86.7 | 63.8 | 0.4 | 8.0 | 17.8 | 82.2 |

conversion of the heavy feedstocks at low reaction temperatures. S/C significantly affected conversion of the feedstocks and distribution of the products, as seen in the results listed in Table 3. At the stoichiometric S/C, the conversions of acetic acid, ethylene glycol, and acetone were rather low, and furthermore, significant amounts of by-products including CO, CH₄, and other complex organic products were produced. Clearly, the decomposition or degradation of the feedstocks occurred to a significant extent at the low steam ratios, which greatly diminished hydrogen yields. Increasing S/C remarkably promoted the efficiency of steam reforming. Both conversion of the feedstocks and selectivity toward H₂ increased substantially. Meanwhile, the amounts of the by-products decreased drastically. The feedstocks and steam

competed for the active sites on catalyst surface in steam reforming process [34]. At high S/C, the high partial pressure of steam in reactor promoted the adsorption of steam on the active sites, and consequently suppressed the decomposition or degradation of the feedstocks. Moreover, the high steam pressure also promoted the water gas shift reaction to remove the CO intermediate, resulting in higher hydrogen selectivity. S/C also showed a remarkable impact on the carbon balance in steam reforming process. It could be seen in Table 3 that the higher the S/C was, the higher the carbon balance was. The formation of the carbon deposit was probably responsible for the large error of the carbon balance at the low S/C, since low steam ratios in reactants favored the decomposition of the feedstocks and led to large

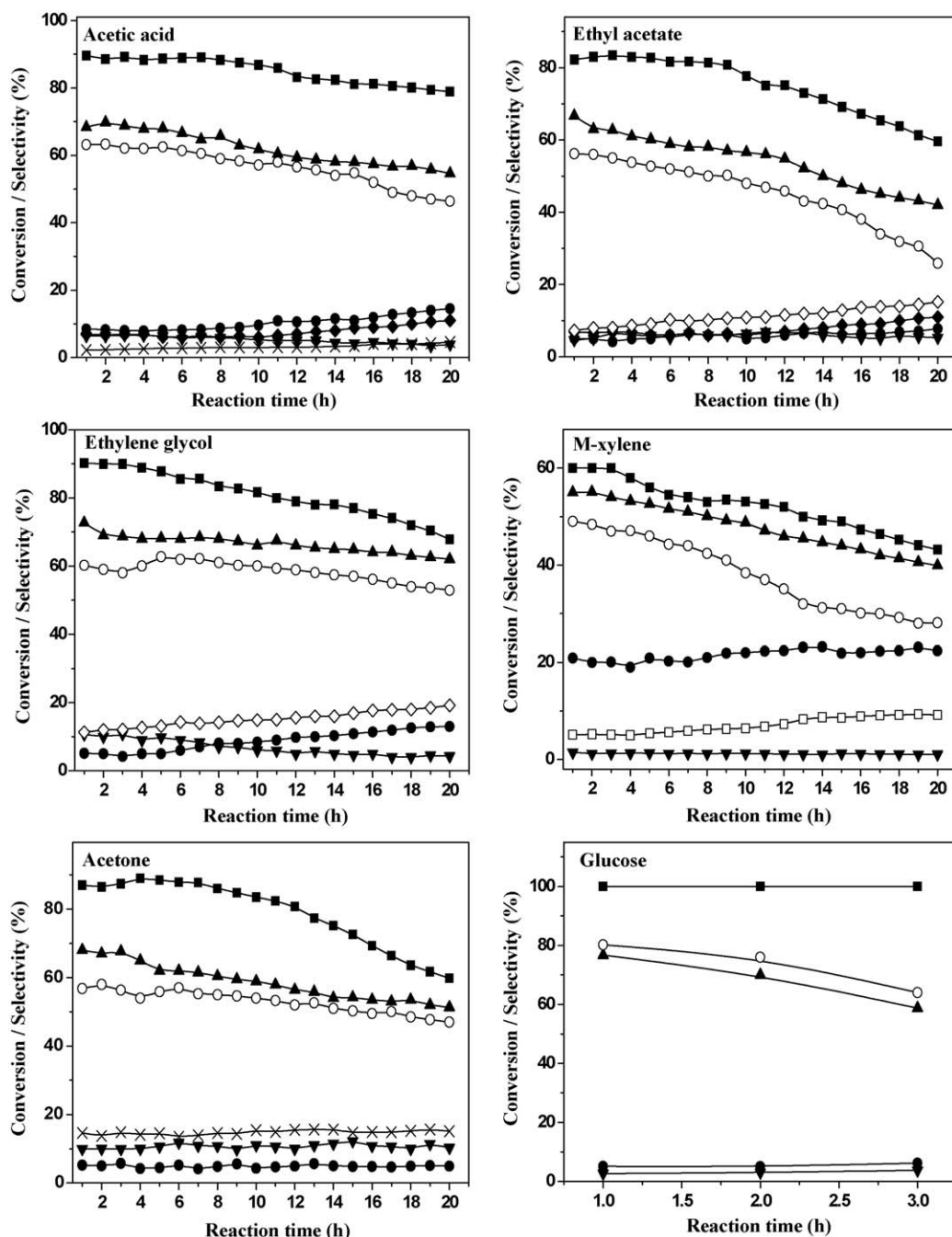


Fig. 4. The endurance tests of the feedstocks reforming: stoichiometric S/C; $T = 600\text{ }^{\circ}\text{C}$; LHSV = 10.1 h^{-1} ; $P = 1\text{ atm.}$; (■) conversion; (▲) H₂; (○) CO₂; (●) CO; (▼) CH₄; (◆) acetone; (◇) ethylene; (×) ketene; (□) benzene.

amounts of by-products that could be potential precursors of coke. Conversely, the production of the carbon precursors (i.e. CO, CH₄) was suppressed while the gasification of the carbon deposit with steam was promoted at the high S/C.

Steam reforming of the heavy feedstocks was carried out at a higher temperature (700 °C). S/C had less influence on conversions of the heavy feedstocks (Table 3), because the higher reaction temperature meant higher rate of steam reforming. Nevertheless, S/C significantly affected the product distribution. At the stoichiometric S/C, large amounts of CO and organic by-products were produced in steam reforming of ethyl acetate and m-xylene. Increasing S/C promoted the water gas shift reaction, the steam reforming of organic by-products, and the gasification of the carbon deposit with steam and CO₂, resulting in the much higher H₂ yield and carbon balance. Nevertheless, the case was a little different for steam reforming of glucose. The carbon balance could not attain 85% even at the S/C of 9, resulting from the severe coke formation in the reforming process. The decomposition of glucose occurred to a significant extent in the steam reforming reaction, leading to the formation of large amount of carbonaceous deposit and the rapid rise of the differential pressure in the system. At the S/C of 3, the progressive accumulation of carbonaceous deposit led to the total blockage of the catalyst bed when the time on stream exceeded only 20 min. Obviously, decomposition of glucose to carbonaceous deposit was the major barrier for its steam reforming. Glucose is unstable at elevated temperature and it will decompose before reaching the catalyst bed, resulting in the serious coke formation in the upper part of the reactor. Therefore, avoiding the decomposition of glucose in the upper part of the reactor is the key to solve the problem of coke formation.

Employing high reaction temperature and high steam ratios can promote the gasification of the coke deposit on catalyst surface with steam or CO₂ in glucose reforming process. However, the coke formation in the upper part of the reactor cannot be thoroughly solved through variation of the reaction parameters. The design of specialized reactor might help to solve the problem. Ramos et al. [35] has designed a reactor that was successfully applied for steam reforming of acetol, a compound that is also unstable at elevated temperatures. The reactor has a lateral arm that can directly feed aqueous solution to catalyst bed. The lateral arm consists of four concentric tubes. The inner tube introduces the aqueous solution to catalyst bed. The second tube provides nitrogen for dispersing the aqueous solution as a spray. The outer tubes are used as a cooling jacket. The merits of the reactor is that preheat of the feedstock in upper part of the reactor is avoided, and consequently prevent the decomposition of the feedstock before the catalyst bed. Therefore, this type of reactor may be applied in glucose reforming and help to solve the problem of coking. In addition to the steam reforming of glucose, the aqueous-phase reforming of glucose [27] and the gasification of glucose in supercritical water [36] were also investigated and were proposed as appropriate ways for conversion of glucose to hydrogen. The main characteristics of these two proposed methods are the low amount of coke formation and the very high pressure in experimental system.

3.4. Coke formation tendency of the feedstocks in the presence or absence steam

Although the catalytic steam reforming of hydrocarbon is often carried out with excess steam (S/C > 3), the catalyst deactivation induced by severe coke deposition invariably affects reformer performance [37]. We therefore carried out the endurance tests under the conditions that deliberately favored coke formation in order to assess the carbon formation tendency of the various feedstocks in steam reforming process. Steam reforming of the

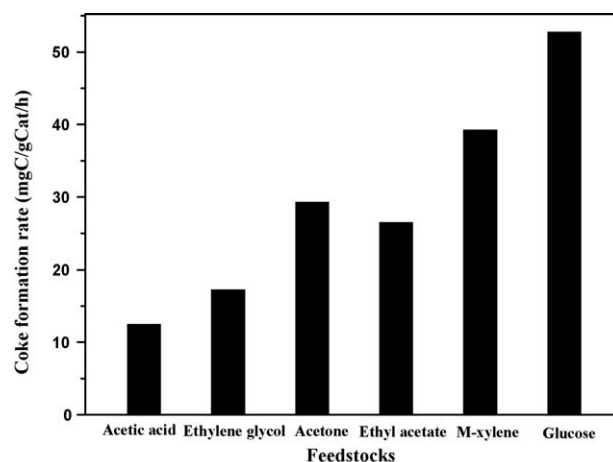


Fig. 5. Coke formation rates of the feedstocks in the presence of steam.

feedstocks was carried out at the stoichiometric S/C and 600 °C for 20 h. Steam reforming of glucose was carried out at a high S/C of 20 because of its high tendency of decomposition to carbonaceous deposit. Conversion of the feedstocks and distribution of the products versus the reaction time as well as the coke formation rates measured by the TG method were summarized in Figs. 4 and 5, respectively.

Coke formation occurred to a different extent in the feedstocks reforming processes, leading to the distinct manners of deactivation of Ni/Al₂O₃ catalyst. The coke formation rates for the feedstocks decreased in the orders: glucose ≫ m-xylene > acetone > ethyl acetate > ethylene glycol > acetic acid. Although the coke formation in acetic acid reforming process was the least significant, acetic acid conversion decreased versus the prolonged reaction time, along with the remarkable increase of CO and acetone selectivities. The low S/C employed in endurance tests favored the production of the by-products that could be the carbon precursors because of the potential occurrence of the disproportionation of CO [38], decomposition of CH₄ [39], and the polymerization of acetone [40]. The carbon formation was more serious in ethylene glycol reforming process. In addition to CO and CH₄, a significant amount of ethylene was detected in steam reforming of ethylene glycol. Ethylene was known as a main source of coke in ethanol reforming reaction, which easily polymerized, forming the polymeric carbon on metal sites [24]. Acetone reforming gave the highest coke formation rate (around 29.3 mgC/(gCat h)) among the light feedstocks investigated. Moreover, the product distribution in acetone reforming process was a little different from those of acetic acid and ethylene glycol reforming. The amount of CO was significant at the initial stage of the endurance tests and increased remarkably with the prolonged reaction time in both acetic acid and ethylene glycol reforming processes. In comparison, CO amount was relatively mild and kept stable in the whole time investigated in acetone reforming process. Therefore, although the production of CO in acetone reforming might contribute to the coke formation, it was not the main reason for the severe coke formation in the endurance test. Acetone showed a high tendency to polymerization to coke at high temperatures [40], and therefore acetone might act as the main source of coke in its steam reforming process because of its high concentration in feed and the high reaction temperature employed.

As for the endurance tests of the heavy feedstocks, lower conversions of the feedstocks and large amounts of by-products were generally observed (Fig. 4). In ethyl acetate reforming process, Ni/Al₂O₃ catalyst deactivated after 9 h of time on stream, resulting from the high coke formation rate (around 26.5 mgC/(gCat h)). Significant amounts of by-products including CO, CH₄, ethylene, and acetone, which all were precursors of coke and might

lead to coke formation, were produced at the end of the test. Ethylene was a typical by-product in ethanol reforming while acetone was a typical by-product in acetic acid reforming. The production of these two by-products agreed well with our previous speculation that ethyl acetate reforming involved the degradation of ethyl acetate to ethoxy and acetyl groups. The by-products in m-xylene reforming, which were mainly CO and benzene, were relatively simple. However, both m-xylene and benzene were the tar compounds and they were easily polymerized and formed carbon deposit on catalyst surface [1,8]. Therefore, the carbon formation in m-xylene reforming process was also significant. Steam reforming of glucose was carried out at the high S/C of 20 with the expectation of gasification of the carbonaceous deposit by the excess steam. Nevertheless, the experiments still terminated after only 3 h of time on stream because of the blockage of the reactor. The amounts of the carbon precursors such as CO, CH₄, and

other organics were little in glucose reforming process. The large amount of carbonaceous deposit mainly derived from the decomposition of glucose.

In addition to glucose, other feedstocks also might decompose directly in reforming process, forming carbonaceous deposit. To measure the coke formation tendency of the feedstocks in absence of steam, we carried out the decomposition experiments using the pure feedstocks with a LHSV of 10.1 h⁻¹ at 600 °C for 3 h. Conversion of the feedstocks and distribution of the products as well as the coke formation rates were depicted in Figs. 6 and 7, respectively. Decomposition of the feedstocks involved the rupture of C–C, C–H, or C–O bonds, resulting in the formation of H₂, carbon-containing compounds, or carbonaceous deposit. The coke formation rates in decomposition of the feedstocks decreased in the orders: m-xylene ≫ ethyl acetate ~ acetone > ethylene glycol > acetic acid. Significant amounts of H₂, CH₄, and benzene were

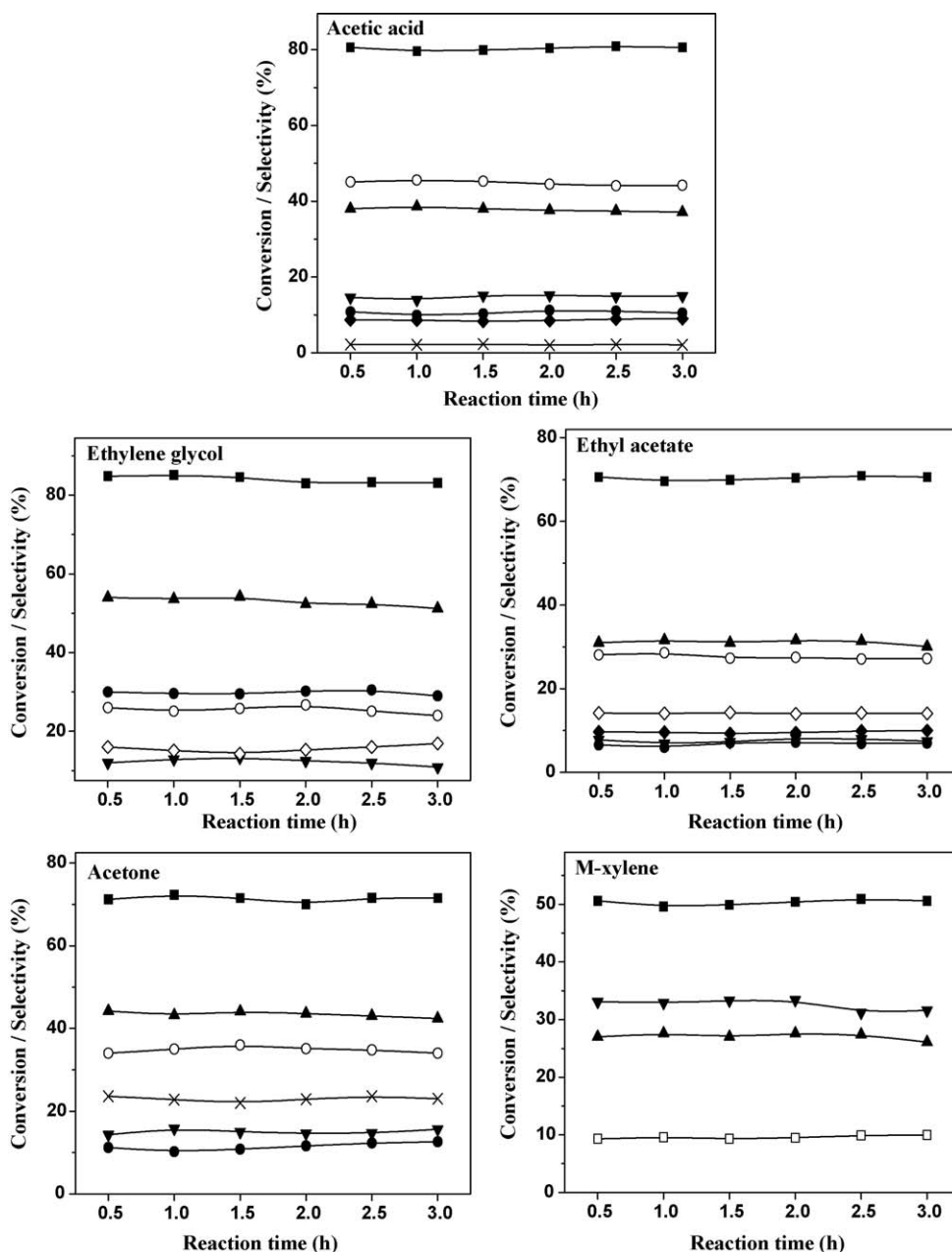


Fig. 6. Decomposition of the feedstocks: $T = 600\text{ }^{\circ}\text{C}$; LHSV = 10.1 h⁻¹; $P = 1\text{ atm.}$; (■) conversion (▲) H₂; (○) CO₂; (●) CO; (▼) CH₄; (◆) acetone; (◇) ethylene; (×) ketene; (□) benzene.

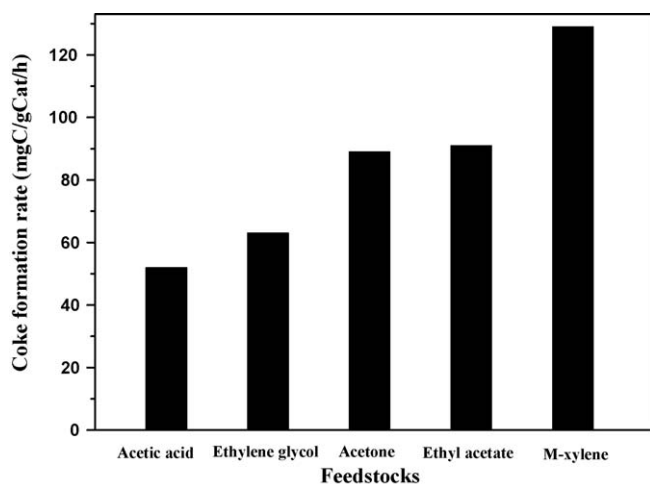


Fig. 7. Coke formation rates of the feedstocks in the absence of steam.

observed in m-xylene decomposition reactions. The decomposition of CH_4 and benzene led to the formation of H_2 and the carbon deposit. Furthermore, m-xylene itself also could decompose to coke and therefore acted as a carbon precursor. The coke deposition in ethyl acetate and acetone decomposition reactions were comparable. This result was slightly different from that in the endurance tests, where the coke formation rate in steam reforming of acetone was higher than that of ethyl acetate. The discrepancy was related to the different reaction pathways. In the presence of steam, the steam reforming competed with the decomposition of ethyl acetate. Comparing the results shown in Figs. 4 and 6, we found the amounts of carbon precursors, ethylene and acetone, were more significant in ethyl acetate decomposition reaction, leading to the more severe coke deposition. In acetone decomposition reaction, both acetone and another ketone compound ketene, which came from the degradation of acetone and also showed a high tendency to polymerization to coke [41], were the sources of coke. The decomposition of ethylene glycol gave significant amounts of CO and ethylene that were the main carbon precursors. In addition, large amount of H_2 was formed in the decomposition reaction. The dehydrogenation associated with the cracking of the C–C bonds of ethylene glycol molecule was responsible for the formation of large amounts of CO and H_2 . As for the decomposition of acetic acid, although the amounts of the by-products, acetone and ketene, were remarkable in the products, acetic acid gave the lowest coke formation rate in the absence of steam (around 52.1 mgC/(gCat h)). Summarizing the results presented above, we found that only ethylene glycol and acetic acid presented relatively low coke formation tendency in absence of steam. Ethylene glycol and acetic acid molecules contain short carbon chain and high content of oxygen. Therefore, decomposition of them was much easier and gave higher concentrations of the oxygenated compounds, and then lower coke formation rates were obtained.

4. Conclusions

Acetic acid, ethylene glycol, and acetone could be efficiently reformed to hydrogen below 500 °C, while much higher temperature was required to convert ethyl acetate and x-xylene. Decomposition of the feedstocks led to formation of organic by-products while the predomination of steam reforming at high temperature and S/C resulted in their elimination. The amount of CH_4 was only significant in the mild temperature region because of the decomposition of the feedstocks and methanation of carbon

oxides. At high temperatures, CO was the main by-product due to the precedence of the reverse water gas shift reaction at this stage.

Glucose, m-xylene, ethyl acetate, and acetone showed high tendency to form coke deposit whether in the presence or absence of steam, due to their instability or high tendency of polymerization at elevated temperatures. Glucose decomposed to a significant extent before reaching the catalyst bed and then was hard to be steam reformed, while steam reforming of ethyl acetate gave large amounts of carbon precursors including ethylene, acetone, and CO. m-Xylene and its degradation product, benzene, were responsible for the severe coke formation, while acetone acted as both the reactant and the carbon precursor in its steam reforming. As for the reforming of ethylene glycol and acetic acid, the by-products such as ethylene, CO, and acetone were the main sources of coke in reforming reactions. To summarize, coke formation is a serious problem in steam reforming reaction. Nevertheless, promotion of steam reforming through optimizing reaction parameters or employing active and coke-resistant catalyst may effectively suppress polymerization of the feedstocks and the production of the carbon precursors, resulting in the elimination of coke deposit.

Acknowledgement

We acknowledge the financial support of the 973 Project of China (No. G 2003CB214503 and 2007CB613305).

References

- [1] J.N. Kuhn, Z. Zhao, L.G. Felix, R.B. Slimane, C.W. Choi, U.S. Ozkan, *Appl. Catal. B: Environ.* 81 (2008) 14.
- [2] A.C. Basagiannis, X.E. Verykios, *Appl. Catal. B: Environ.* 82 (2008) 77.
- [3] Y. Ma, Y. Xu, M. Demura, T. Hirano, *Appl. Catal. B: Environ.* 80 (2008) 15.
- [4] A. Denis, W. Grzegorzczak, W. Gac, A. Machocki, *Catal. Today* 137 (2008) 453.
- [5] S. Gudlavalleti, T. Ros, D. Lieftink, *Appl. Catal. B: Environ.* 74 (2007) 251.
- [6] A. Birot, F. Epron, C. Descorme, D. Duprez, *Appl. Catal. B: Environ.* 79 (2008) 17.
- [7] G.B. Sun, K. Hidajat, X.S. Wu, S. Kawi, *Appl. Catal. B: Environ.* 81 (2008) 303.
- [8] D. Swierczynski, S. Libs, C. Courson, A. Kiennemann, *Appl. Catal. B: Environ.* 74 (2007) 211.
- [9] K.D. Panopoulos, L.E. Fryda, J. Karl, S. Poulou, E. Kakaras, *J. Power Sources* 159 (2006) 570.
- [10] T. Davidian, N. Guilhaume, E. Iojoiu, H. Provendier, C. Mirodatos, *Appl. Catal. B: Environ.* 73 (2007) 116.
- [11] S. Rioche, S. Kulkarni, F.C. Meunier, J.P. Breen, R. Burch, *Appl. Catal. B: Environ.* 61 (2005) 130.
- [12] A. Oasmaa, D. Meier, in: A.V. Bridgwater (Ed.), *Fast Pyrolysis of Biomass: A Handbook*, vol. 2, CPL Press, Newbury, UK, 2002, pp. 41–58.
- [13] J. Piskorz, S.D. Scott, D. Radlein, in: E.J. Soltes, T.A. Milne (Eds.), *Pyrolysis Oils from Biomass: Producing, Analyzing and Upgrading*, ACS Symposium Series 376, American Chemical Society, Washington, DC, 1988, pp. 167–178.
- [14] J.R. Galdamez, L. Garcia, R. Bilbao, *Energy Fuels* 19 (2005) 1133.
- [15] F. Bimbela, M. Oliva, J. Ruiz, L. Garcia, J. Arauzo, J. Anal. *Appl. Pyrol.* 79 (2007) 112.
- [16] X. Hu, G. Lu, *J. Mol. Catal. A: Chem.* 261 (2007) 43.
- [17] P.N. Kechagiopoulos, S.S. Voutetakis, A.A. Lemonidou, I.A. Vasalos, *Catal. Today* 127 (2007) 246.
- [18] M. Turco, G. Bagnasco, C. Cammarano, P. Senese, U. Costantino, M. Sisani, *Appl. Catal. B: Environ.* 77 (2007) 46.
- [19] B. Zhang, X. Tang, Y. Li, Y. Xu, W. Shen, *Int. J. Hydrogen Energy* 32 (2007) 2367.
- [20] V.V. Galvita, G.L. Semin, V.D. Belyaev, T.M. Yurieva, V.A. Sobyannin, *Appl. Catal. A: Gen.* 216 (2001) 85.
- [21] X. Wang, R.J. Gorte, *Appl. Catal. A: Gen.* 224 (2002) 209.
- [22] M. Marquovich, S. Czernik, E. Chornet, D. Montane, *Energy Fuels* 13 (1999) 1160.
- [23] K. Faungnawakij, Y. Tanaka, N. Shimoda, T. Fukunaga, R. Kikuchi, K. Eguchi, *Appl. Catal. B: Environ.* 74 (2007) 144.
- [24] M. Ni, D.Y.C. Leung, M.K.H. Leung, *Int. J. Hydrogen Energy* 32 (2007) 3238.
- [25] A.C. Basagiannis, X.E. Verykios, *Int. J. Hydrogen Energy* 32 (2007) 3343.
- [26] S. Adhikari, S. Fernando, A. Haryanto, *Energy Fuels* 21 (2007) 2306.
- [27] R.R. Davda, J.W. Shabaker, G.W. Huber, R.D. Cortright, J.A. Dumesic, *Appl. Catal. B: Environ.* 56 (2005) 171.
- [28] K. Eguchi, N. Shimoda, K. Faungnawakij, T. Matsui, R. Kikuchi, S. Kawashima, *Appl. Catal. B: Environ.* 80 (2008) 156.
- [29] S.K. Shin, S.K. Kim, H.L. Kim, C.R. Park, *J. Photochem. Photobiol. A: Chem.* 143 (2001) 11.
- [30] A.P. Farkas, F. Solymosi, *Surf. Sci.* 602 (2008) 1475.
- [31] I. Czekaj, F. Loviat, F. Raimondi, J. Wambach, S. Biollaz, A. Wokaun, *Appl. Catal. A: Gen.* 329 (2007) 68.
- [32] C.W. Hu, J. Yao, H.Q. Yang, Y. Chen, A.M. Tian, *J. Catal.* 166 (1997) 1.

- [33] S.H. Kim, S.W. Nam, T.H. Lim, H.I. Lee, *Appl. Catal. B: Environ.* 81 (2008) 97.
- [34] M. Marquevich, F. Medina, D. Montane, *Catal. Commun.* 2 (2001) 119.
- [35] M.C. Ramos, A.I. Navascues, L. Garcia, R. Bilbao, *Ind. Eng. Chem. Res.* 46 (2007) 2399.
- [36] Y.J. Lu, L.J. Guo, C.M. Ji, X.M. Zhang, X.H. Hao, Q.H. Yan, *Int. J. Hydrogen Energy* 31 (2006) 822.
- [37] K.M. Hardiman, T.T. Ying, A.A. Adesina, E.M. Kennedy, B.Z. Dlugogorski, *Chem. Eng. J.* 102 (2004) 119.
- [38] D.L. Trimm, *Catal. Today* 49 (1999) 3.
- [39] J. Guo, H. Lou, X. Zheng, *Carbon* 45 (2007) 1314.
- [40] B. Zhang, X. Tang, Y. Li, W. Cai, Y. Xu, W. Shen, *Catal. Commun.* 7 (2006) 367.
- [41] H. Egret, J. Couvercelle, J. Belleney, C. Bunel, *Eur. Polym. J.* 38 (2002) 1953.